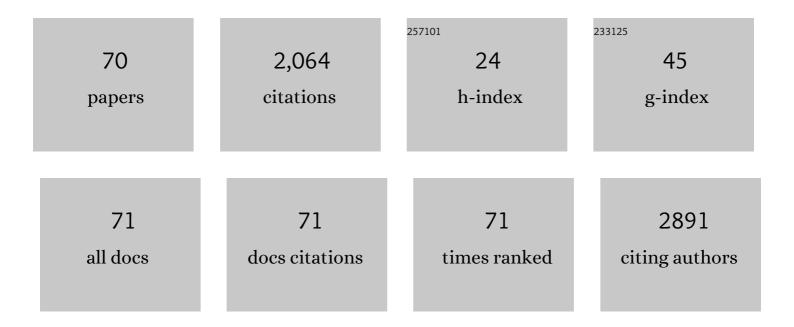
## Kai Chen

List of Publications by Year in descending order

Source: https://exaly.com/author-pdf/3191449/publications.pdf Version: 2024-02-01



KALCHEN

#	Article	IF	CITATIONS
1	Dual-Band Perfect Absorber for Multispectral Plasmon-Enhanced Infrared Spectroscopy. ACS Nano, 2012, 6, 7998-8006.	7.3	459
2	Infrared Perfect Absorbers Fabricated by Colloidal Mask Etching of Al–Al <sub>2</sub> O <sub>3</sub> –Al Trilayers. ACS Photonics, 2015, 2, 964-970.	3.2	172
3	Infrared Aluminum Metamaterial Perfect Absorbers for Plasmonâ€Enhanced Infrared Spectroscopy. Advanced Functional Materials, 2015, 25, 6637-6643.	7.8	129
4	Hole Array Perfect Absorbers for Spectrally Selective Midwavelength Infrared Pyroelectric Detectors. ACS Photonics, 2016, 3, 1271-1278.	3.2	92
5	Moiré Nanosphere Lithography. ACS Nano, 2015, 9, 6031-6040.	7.3	91
6	Plasmon-Enhanced Second-Harmonic Generation from Ionic Self-Assembled Multilayer Films. Nano Letters, 2007, 7, 254-258.	4.5	81
7	Spectrally Selective Midâ€Infrared Thermal Emission from Molybdenum Plasmonic Metamaterial Operated up to 1000 °C. Advanced Optical Materials, 2016, 4, 1987-1992.	3.6	79
8	Solar water heating and vaporization with silicon nanoparticles at mie resonances. Optical Materials Express, 2016, 6, 640.	1.6	69
9	Anapole mediated giant photothermal nonlinearity in nanostructured silicon. Nature Communications, 2020, 11, 3027.	5.8	69
10	Restricted meniscus convective self-assembly. Journal of Colloid and Interface Science, 2010, 344, 315-320.	5.0	55
11	High-sensitivity and fast-response fiber-tip Fabry–Pérot hydrogen sensor with suspended palladium-decorated graphene. Nanoscale, 2019, 11, 15821-15827.	2.8	49
12	High quality thermochromic VO2 films prepared by magnetron sputtering using V2O5 target with in situ annealing. Applied Surface Science, 2019, 495, 143436.	3.1	44
13	Tunable Nanoantennas for Surface Enhanced Infrared Absorption Spectroscopy by Colloidal Lithography and Post-Fabrication Etching. Scientific Reports, 2017, 7, 44069.	1.6	37
14	Effect of different surfactants on structural and optical properties of Ce3+ and Tb3+ co-doped BiPO4 nanostructures. Optical Materials, 2015, 39, 110-117.	1.7	34
15	Resonant Optical Absorption and Photothermal Process in High Refractive Index Germanium Nanoparticles. Advanced Optical Materials, 2017, 5, 1600902.	3.6	34
16	Ultra-Broadband Directional Scattering by Colloidally Lithographed High-Index Mie Resonant Oligomers and Their Energy-Harvesting Applications. ACS Applied Materials & Interfaces, 2018, 10, 16776-16782.	4.0	34
17	Photocurrent Enhancements of TiO <sub>2</sub> -Based Nanocomposites with Gold Nanostructures/Reduced Graphene Oxide on Nanobranched Substrate. Journal of Physical Chemistry C, 2019, 123, 21103-21113.	1.5	33
18	Ultra-Narrow Band Mid-Infrared Perfect Absorber Based on Hybrid Dielectric Metasurface. Nanomaterials, 2019, 9, 1350.	1.9	30

Kai Chen

#	Article	IF	CITATIONS
19	Structure and optical properties of sputter deposited pseudobrookite Fe <sub>2</sub> TiO <sub>5</sub> thin films. CrystEngComm, 2019, 21, 34-40.	1.3	30
20	Tunable multiband metasurfaces by moiré nanosphere lithography. Nanoscale, 2015, 7, 20391-20396.	2.8	29
21	Angle-and polarization-dependent collective excitation of plasmonic nanoarrays for surface enhanced infrared spectroscopy. Optics Express, 2011, 19, 11202.	1.7	27
22	Ultra-narrow-band metamaterial perfect absorber based on surface lattice resonance in a WS <sub>2</sub> nanodisk array. Optics Express, 2021, 29, 27084.	1.7	27
23	Active molecular plasmonics: tuning surface plasmon resonances by exploiting molecular dimensions. Nanophotonics, 2015, 4, 186-197.	2.9	26
24	Robust dithiocarbamate-anchored amine functionalization of Au nanoparticles. Journal of Nanoparticle Research, 2011, 13, 751-761.	0.8	24
25	Proteinâ€Functionalized Indiumâ€Tin Oxide Nanoantenna Arrays for Selective Infrared Biosensing. Advanced Optical Materials, 2017, 5, 1700091.	3.6	23
26	High- <i>Q</i> , low-mode-volume and multiresonant plasmonic nanoslit cavities fabricated by helium ion milling. Nanoscale, 2018, 10, 17148-17155.	2.8	22
27	Dual-band <i>in situ</i> molecular spectroscopy using single-sized Al-disk perfect absorbers. Nanoscale, 2019, 11, 9508-9517.	2.8	22
28	Selective patterned growth of ZnO nanowires/nanosheets and their photoluminescence properties. Optical Materials Express, 2015, 5, 353.	1.6	21
29	Cylindrical vector beams reveal radiationless anapole condition in a resonant state. Opto-Electronic Advances, 2022, 5, 210014-210014.	6.4	21
30	Selective thermal emitters with infrared plasmonic indium tin oxide working in the atmosphere. Optical Materials Express, 2019, 9, 2534.	1.6	20
31	Flexible microbubble-based Fabry–Pérot cavity for sensitive ultrasound detection and wide-view photoacoustic imaging. Photonics Research, 2020, 8, 1558.	3.4	19
32	Electromechanically Tunable Suspended Optical Nanoantenna. Nano Letters, 2016, 16, 2680-2685.	4.5	18
33	Excitation Induced Tunable Emission in Ce <sup><b>3+</b></sup> /Eu <sup><b>3+</b></sup> Codoped BiPO <sub><b>4</b></sub> Nanophosphors. Journal of Spectroscopy, 2015, 2015, 1-10.	0.6	14
34	Rayleigh anomaly-enabled mode hybridization in gold nanohole arrays by scalable colloidal lithography for highly-sensitive biosensing. Nanophotonics, 2022, 11, 507-517.	2.9	14
35	Far-field and near-field monitoring of hybridized optical modes from Au nanoprisms suspended on a graphene/Si nanopillar array. Nanoscale, 2017, 9, 16950-16959.	2.8	10
36	Effects of nanoscale morphology and defects in oxide: optoelectronic functions of zinc oxide nanowires. Radiation Effects and Defects in Solids, 2016, 171, 22-33.	0.4	9

Kai Chen

#	Article	IF	CITATIONS
37	Enhanced photocurrent generation from indium–tin-oxide/Fe2TiO5 hybrid nanocone arrays. Nano Energy, 2020, 76, 104965.	8.2	9
38	Transparent oxides forming conductor/insulator/conductor heterojunctions for photodetection. Nanotechnology, 2015, 26, 215203.	1.3	8
39	Morphology Effect of Bismuth Vanadate on Electrochemical Sensing for the Detection of Paracetamol. Nanomaterials, 2022, 12, 1173.	1.9	8
40	Band-rejection and bandpass filters based on mechanically induced long-period fiber gratings. Microwave and Optical Technology Letters, 2004, 42, 15-17.	0.9	7
41	Interface effects in plasmon-enhanced second-harmonic generation from self-assembled multilayer films. Journal of the Optical Society of America B: Optical Physics, 2010, 27, 92.	0.9	7
42	Cylindrical vector beam revealing multipolar nonlinear scattering for superlocalization of silicon nanostructures. Photonics Research, 2021, 9, 950.	3.4	7
43	Plasmon mediated cathodic photocurrent generation in sol-gel synthesized doped SrTiO3 nanofilms. APL Materials, 2015, 3, .	2.2	6
44	Indium–Tin–Oxide Nanostructures for Plasmon-Enhanced Infrared Spectroscopy: A Numerical Study. Micromachines, 2019, 10, 241.	1.4	6
45	Etching-free high-throughput intersectional nanofabrication of diverse optical nanoantennas for nanoscale light manipulation. Journal of Colloid and Interface Science, 2022, 622, 950-959.	5.0	6
46	Nanoantenna Structure with Mid-Infrared Plasmonic Niobium-Doped Titanium Oxide. Micromachines, 2020, 11, 23.	1.4	5
47	Sunlight absorbing titanium nitride nanoparticles. , 2015, , .		4
48	Enhanced Multiphoton-Induced Luminescence in Silver Nanoparticles Fabricated with Nanosphere Lithography. Plasmonics, 2015, 10, 87-98.	1.8	4
49	A novel interleaver based on dual-pass Mach-Zehnder interferometer. Microwave and Optical Technology Letters, 2004, 42, 253-255.	0.9	3
50	Loss-favored ultrasensitive refractive index sensor based on directional scattering from a single all-dielectric nanosphere. Journal of Materials Chemistry C, 2020, 8, 6350-6357.	2.7	3
51	Ensemble of gold-patchy nanoparticles with multiple hot-spots for plasmon-enhanced vibrational spectroscopy. Proceedings of SPIE, 2016, , .	0.8	2
52	Mass Fabrication of WS <sub>2</sub> Nanodisks and their Scattering Properties. Advanced Materials Technologies, 0, , 2200432.	3.0	2
53	Aluminum infrared plasmonic perfect absorbers fabricated by colloidal lithography. , 2015, , .		1
54	Moiré nanosphere lithography: use colloidal moiré patterns as masks. Proceedings of SPIE, 2015, , .	0.8	1

KAI CHEN

#	Article	IF	CITATIONS
55	Aluminum infrared plasmonic perfect absorbers for wavelength selective devices. Proceedings of SPIE, 2016, , .	0.8	1
56	UV-visible light photocurrent enhancement in STO thin films through metal-defect co-doping effect combined with Au plasmons. Materials Express, 2017, 7, 66-71.	0.2	1
57	Metal/Conductive Oxide Plasmonic Structures for Surface-Enhanced Infrared Absorption Spectroscopy. Bunseki Kagaku, 2018, 67, 81-94.	0.1	1
58	High Temperature Wavelength-Selective Thermal Emitters Based on Metal-Insulator-Metal Structures. Hyomen Kagaku, 2016, 37, 380-385.	0.0	1
59	Effect of the Interface in Plasmon-enhanced Second Harmonic Generation from Nonlinear Optical Thin Films. Materials Research Society Symposia Proceedings, 2010, 1248, 1120.	0.1	0
60	The Relationship between Growth Speed and Ambient Humidity in Convective Self-assembly. Materials Research Society Symposia Proceedings, 2010, 1273, 10701.	0.1	0
61	Thin and Robust Encapsulation of Silver and Gold Nanoparticles with Dithiocarbamate-anchored Polyelectrolytes. Materials Research Society Symposia Proceedings, 2011, 1348, 140001.	0.1	0
62	Integrated plasmonic nanobiosensors. , 2013, , .		0
63	Large Area, Aluminum Metal-Insulator-Metal Infrared Perfect Absorber. , 2014, , .		0
64	Large-area Tunable Al Plasmonic Substrate for Infrared Spectroscopy. , 2014, , .		0
65	Lossy plasmonic resonances in nanoparticles for broadband light absorption. , 2015, , .		0
66	Fabrication and Characterization of Moir $\tilde{A}$ ${\ensuremath{\mathbb C}}$ Metasurfaces. , 2016, , .		0
67	Nanowire-plasmonic photocatalysts and thermal emitters. , 2017, , .		0
68	Ultra-narrow Nanoslit Cavities for High-Q Resonances in the Visible Range. , 2018, , .		0
69	Enhanced photoelectrochemical water splitting by plasmonic Au nanostructures/reduced graphene oxide. , 2018, , .		0
70	Al nanoantennas for plasmon-enhanced infrared spectroscopy. , 2018, , .		0